

1 Effects of colonization asymmetries
2 on metapopulation persistence

3 Séverine Vuilleumier^{*,1}, Benjamin M. Bolker², Olivier Lévêque³

4 Running title: Metapopulation persistence with colonization asymmetries

5 ¹ Department of Ecology and Evolution

6 University of Lausanne

7 CH-1015 Lausanne

8 Switzerland

9 Phone: +41 21 692 4176

10 Fax: +41 21 692 4165

11 severine.vuilleumier@unil.ch

12 ² Biology Department

13 University of Florida

14 Box 118525

15 Gainesville, FL 32611-8525

16 USA

17 Phone: (352) 392-5697

18 Fax: (352) 392-3704

19 bolker@ufl.edu

20 ³ Laboratoire de Théorie de l'Information (LTHI)

21 École Polytechnique Fédérale de Lausanne (EPFL)

22 Bâtiment INR, Station 14

23 1015 Lausanne, Switzerland

24 Phone: + 41 21 693 81 12

25 Fax: + 41 21 893 76 98

26 olivier.leveque@epfl.ch

27 * Corresponding author

1 **Abstract**

2 Ocean currents, prevailing winds, and the hierarchical structures of river networks are
3 known to create asymmetries in re-colonization between habitat patches. The impacts of
4 such asymmetries on metapopulation persistence are seldom considered, especially rarely
5 in theoretical studies. Considering three classical models (the island, the stepping stone
6 and the distance-dependent model), we explore how metapopulation persistence is af-
7 fected by (i) asymmetry in dispersal strength, in which the colonization rate between
8 two patches differs in direction, and (ii) asymmetry in connectivity in which the overall
9 colonization pattern displays asymmetry (circulating or dendritic networks). Viability
10 can be drastically reduced when directional bias in dispersal strength is higher than 25%.
11 Re-colonization patterns that allow for strong local connectivity provide the highest per-
12 sistence compared to systems that allow circulation. Finally, asymmetry has relatively
13 weak effects when metapopulations maintain strong general connectivity.

14

15 *Keywords:* Asymmetric dispersal, colonization, persistence, metapopulation capacity of
16 a fragmented landscape, model.

1. Introduction

Most models of metapopulation dynamics assume that dispersal between patches is symmetric — i.e., that for any pair of patches, the probability of interpatch dispersal and hence the recolonization probability is the same in both directions. Most of the literature on dispersal asymmetry focuses on source-sink metapopulation dynamics, which arise from variation in productivity of populations (Pulliam, 1988; Morris, 1991; Kawecki and Stearns, 1993; Kawecki, 1995; Holt, 1996; Saether et al., 1999; Kawecki and Holt, 2002). Directional dispersal resulting from heterogeneity (due to environmental gradients such as prevailing winds, ocean and river currents) is also well known to affect the symmetry of colonization processes between populations (Largier, 2003; Schooley and Wiens, 2003; Levin, 2006; Thorrold, 2006; Cheal et al., 2007; Bay et al., 2008). In particular, ecologists have documented asymmetric dispersal patterns for freshwater fish populations (Bolnick et al., 2008) for marine and riverine invertebrates (Lutscher et al., 2007; Bay et al., 2008; Young et al., 2008), and for various plant species (Friedman and Stein, 1980; Keddy, 1981; Watkinson, 1985; Gornall et al., 1998; Imbert and Lefèvre, 2003).

Spatial heterogeneity can also create asymmetric patterns in the spatial distribution of connectivity among populations, as well as asymmetries in re-colonization rates between pairs of patches. For example, the fractal and hierarchical structure of river networks creates sub-structures (tributaries) that are strongly locally connected through river segments that allows only colonization in some direction. Such dendritic networks are found in watersheds and cave ecosystems as well as in river networks (Fagan, 2002; Benda et al., 2004; Finn et al., 2006; Labonne et al., 2008). Similarly, marine species are expected to disperse under the influence of ocean currents or depending on current bifurcations and large scale movement of water (Caley et al., 1996). Studies of a variety of empirical systems have shown that island and isolation-by distance metapopulation models with homogeneous re-colonization patterns cannot capture the dynamics, nor the genetic structure, of such metapopulations (Gaines et al., 2003; Bode et al., 2006; Bay et al., 2008; Labonne et al., 2008; Muneeppeerakul et al., 2008; Chaput-Bardy et al., 2009; Hughes et al., 2009). Although there is considerable evidence for various forms of asymmetry in re-colonization, the properties of metapopulation persistence under these conditions have

1 been poorly explored. The few models that have considered asymmetric re-colonization
2 pattern make the simplifying assumption that the number of patches is very small, usu-
3 ally two (Pulliam and Danielson, 1991; Kawecki and Holt, 2002; Amarasekare, 2004), or
4 that the asymmetry is either very weak (Ovaskainen, 2003) or complete (Vuilleumier and
5 Possingham, 2006).

6 We consider here two types of asymmetries: *asymmetry in dispersal strength* and *asym-*
7 *metry in connectivity*. Asymmetry in dispersal strength describes the situation where the
8 colonization rate from a patch i to a patch j and the colonization rate in the reverse
9 direction, from patch j to patch i , differ in strength. These differences could be due
10 to environmental gradients (e.g. wind, ocean currents) that favor dispersal in one di-
11 rection. We define an asymmetry factor $0 \leq d \leq 1/2$ that characterizes the fraction of
12 colonization that occurs in the unfavored direction. Under asymmetry in connectivity,
13 the re-colonization rate in either direction between any two connected patches is either
14 identical or perfectly asymmetric, but the global arrangement of connections has a di-
15 rectional bias that ranges from 0 (all asymmetric connections are oriented in the same
16 direction, “downwind”) to $1/2$ (asymmetric connections are oriented at random).

17 These two variants of re-colonization asymmetries are applied to three classical models:
18 the *island model*, where re-colonization probabilities are identical between any two given
19 habitat patches; the *stepping stone model*; where empty habitat patches can only be
20 re-colonized by neighboring occupied patches; and the *distance-dependent model*, where
21 re-colonization probabilities are assumed to decay exponentially with the inter-patch
22 distance.

23 We first define the connectivity matrix resulting from the various colonization models
24 considered. Second, following Ovaskainen and Hanski (2001), we estimate the metapop-
25 ulation capacity, which corresponds to the leading eigenvalue of the connectivity matrix,
26 for each case considered. Analytical solutions are presented when possible (for most cases
27 of asymmetry in dispersal strength); otherwise we compute eigenvalues numerically. We
28 then run stochastic simulations in order to estimate extinction probabilities and to ex-
29 plore the relationship between metapopulation capacity and extinction when the number
30 of habitat patches is finite and environmental stochasticity affects the rate of extinction
31 and colonization.

1 We demonstrate that asymmetries can drastically affect metapopulation capacity and
2 persistence and provide recommendations on the use of metapopulation models to esti-
3 mate persistence when asymmetry in recolonization pattern is expected.

4 **2. Methods**

5 *2.1. Metapopulation models*

6 Metapopulation persistence depends on the balance between the probability of local
7 population extinction and the re-colonization of empty habitat patches (Levin, 1969;
8 Hanski, 1999). The dynamics of a metapopulation were first described by Levins (1969,
9 1970) in a continuous-time, deterministic *island model*, which considers n equivalent
10 patches having an equal probability of colonizing any of the $n - 1$ other patches. The
11 change in expected fraction of occupied patches p is determined by the local extinction
12 rate (e) and the colonization rate (c). It follows that

$$\frac{dp}{dt} = cp(1 - p) - ep, \quad (1)$$

13 which has a globally stable fixed point when

$$p^* = 1 - \frac{e}{c} > 0 \quad (2)$$

14 This model assumes a uniform re-colonization pattern in which each habitat patch has
15 the same probability of re-colonization. A variant of the Levins model proposed by Hanski
16 and Gyllenberg (1997) considers the re-colonization pattern as the product cM , where c
17 is the colonization rate of the focal species and the matrix M describes the re-colonization
18 pattern. In this $n \times n$ matrix, the element m_{ij} characterizes the probability of colonization
19 from habitat patch i to habitat patch j . Under the island model, $m_{ij} = 1$ for all $i \neq j$. If
20 we instead assume that colonization can only occur to and from neighboring patches, we
21 obtain a *stepping stone model* (Kimura and Weiss, 1964) and the element of the matrix
22 M , m_{ij} will be different from zero only if $|i - j| = 1$. In this case, a metapopulation can
23 persist if

$$(1 - e)Rc > e \quad (3)$$

1 (Durrett and Levin, 1994), where R is the number of neighboring populations. This
 2 condition also applies to a two-dimensional lattice model (Durrett and Levin, 1994).

3 Considering spatially distributed populations in which colonization decreases exponen-
 4 tially with distance, we have (Hanski, 1999):

$$m_{ij} = \begin{cases} \exp(-\alpha d_{ij}) & \text{if } i \neq j \\ 0 & \text{if } i = j \end{cases} \quad (4)$$

5 where d_{ij} is the distance between the habitat patches and $\alpha = 1/h$ sets the migration
 6 range of the focal species with h its mean dispersal distance. As α increases, the species
 7 dispersal range decreases.

8 The deterministic equation describing the evolution of the state of the system is given
 9 in Ovaskainen and Hanski (2001) for a discrete-time model:

$$p_j(t+1) - p_j(t) = c \left(\sum_i m_{ij} p_i(t) \right) (1 - p_j(t)) - e p_j(t) \quad (5)$$

10 where $p_j(t)$ denotes the probability that patch j is occupied at time t . Note that equa-
 11 tion (5) is only accurate if the occupancy probabilities in different patches are temporally
 12 uncorrelated. For a system with a large number of patches, in which each habitat patch
 13 contributes equally to the dynamics of the system, equation (1) provides a good approx-
 14 imation to equation (5).

15 Ovaskainen and Hanski (2001) show that in the case where the matrix M is irreducible,
 16 an equilibrium solution $p^* > 0$ to the above equation exists if and only if

$$\lambda_M > \frac{e}{c} \quad (6)$$

17 where λ_M is the largest eigenvalue of the matrix M .

18 Our main object of investigation in the following is twofold. First, we will study in
 19 detail, for the various models considered, the behavior of the largest eigenvalue of the
 20 landscape matrix M . Second, we will compare the viability threshold (6), obtained with
 21 the deterministic model of Ovaskainen and Hanski (2001), to that obtained numerically
 22 with a simple stochastic model of extinctions and colonizations.

1 2.2. Defining patterns of asymmetry

2 2.2.1. Asymmetry in dispersal strength

3 We characterize the asymmetry in dispersal strength by a factor d , varying from 0
4 (complete asymmetry) to $1/2$ (complete symmetry). If c is the total colonization rate from
5 a given patch, then $c(1 - d)$ represents the total colonization rate in the main direction
6 of colonization and cd represents the total colonization rate in the other direction.

7 To allow comparison of the impact of asymmetry in the island model, the stepping
8 stone model and the distance-dependent model, we normalize the largest eigenvalue of
9 the adjacency matrix M . Thus, we assume that the largest row-sum of the matrix M
10 approaches 1 for large system size (and also that $m_{ii} = 0$ for all i). Under this normal-
11 ization condition, the largest eigenvalue of M also approaches 1 in the symmetric case.
12 In practically all the situations considered in this section, the matrix M is irreducible, so
13 condition (6) applies. The only exception arises in extreme cases where the matrix M is
14 completely asymmetric (i.e. there is no cycle in the graph of patch connections), in which
15 case extinction occurs with probability one, regardless of the system parameters.

16 In the remainder of this section (except for the grid stepping stone model) we assume
17 that the landscape matrix M has a *Toeplitz structure*, that is, $m_{ij} = f(i - j)$ for some
18 function f (see Gray 2006). The choice of the function f depends on the model considered
19 (stepping stone, island or distance-dependent model) and the asymmetry introduced in
20 the model. In order to investigate the impact of asymmetry, we further assume that

$$m_{ij} = \begin{cases} f_+(|i - j|) & \text{if } j > i \\ 0 & \text{if } i = j \\ f_- (|i - j|) & \text{if } i > j \end{cases} \quad (7)$$

21 where f_+ , f_- are non-negative and decreasing functions on the set of positive integers
22 obeying the following normalization conditions:

$$\lim_{n \rightarrow \infty} \sum_{k=1}^{n/2} f_+(k) = d \quad \text{and} \quad \lim_{n \rightarrow \infty} \sum_{k=1}^{n/2} f_-(k) = 1 - d \quad (8)$$

23 where d is the asymmetry factor of the model. Notice that as $d \in [0, 1/2]$, the main
24 direction of colonization under this model is the direction associated with the decay

1 function f_- . Condition (8) ensures that the largest row-sum of the matrix M for large
 2 system size n tends to 1.

3 *Island model.* In the island model, assuming that all habitat patches can be re-colonized
 4 from any other occupied habitat patch, we set

$$f_+(k) = d/Z \quad \forall k \geq 1 \quad \text{and} \quad f_-(k) = (1-d)/Z \quad \forall k \geq 1 \quad (9)$$

5 where the normalization constant Z is taken to be $Z = n/2$, which ensures that condition
 6 (8) is satisfied. This leads to the matrix model

$$m_{ij} = \begin{cases} d/Z & \text{if } j > i \\ 0 & \text{if } i = j \\ (1-d)/Z & \text{if } i > j \end{cases} \quad (10)$$

7 *Stepping stone model.* In the stepping stone model, assuming that only neighboring habi-
 8 tat patches can be re-colonized, we have

$$f_+(k) = d \quad \text{if } k = 1 \quad \text{and} \quad f_+(k) = 0 \quad \text{otherwise} \quad (11)$$

9 and

$$f_-(k) = 1-d \quad \text{if } k = 1 \quad \text{and} \quad f_-(k) = 0 \quad \text{otherwise} \quad (12)$$

10 which leads to the matrix model

$$m_{ij} = \begin{cases} d & \text{if } j = i + 1 \\ 1-d & \text{if } i = j + 1 \\ 0 & \text{otherwise} \end{cases} \quad (13)$$

11 *Distance-dependent models.* To investigate the distance-dependent model, we focus on a
 12 model in which the colonization rate decreases exponentially with the ratio of the distance
 13 between habitat patches $|i - j|$ normalized by the average colonization distance h of the
 14 species in focus, as suggested by Hanski (1999). Additionally, for this model, we apply
 15 two forms of asymmetry: weak and strong asymmetry, that differ in the following sense:

1 while the first model only favors the dispersal strength in one direction, the second one
 2 also creates a bias in the average colonization distances (see Figure 1).

3 Under the *weakly asymmetric distance-dependent model*, the asymmetry factor d only
 4 enters into the matrix M as a weighting factor, as in the previously studied models.
 5 Asymmetry translates into a shift in the strength of colonization in one direction compare
 6 to the other. More precisely, we have

$$f_+(k) = d \exp(-\alpha k)/Z \quad \forall k \geq 1 \quad \text{and} \quad f_-(k) = (1-d) \exp(-\alpha k)/Z \quad \forall k \geq 1 \quad (14)$$

7 where $\alpha = 1/h > 0$ and the normalization constant Z is given by

$$Z = \sum_{k=1}^{\infty} \exp(-\alpha k) = \frac{e^{-\alpha}}{1 - e^{-\alpha}} \quad (15)$$

8 in order to ensure that condition (8) is satisfied. This leads the following matrix model

$$m_{ij} = \begin{cases} d \exp(-\alpha |i-j|)/Z & \text{if } j > i \\ 0 & \text{if } i = j \\ (1-d) \exp(-\alpha |i-j|)/Z & \text{if } i > j \end{cases} \quad (16)$$

9 In this case, it should be noted that the average colonization distance h is the same in
 10 both directions; only the strength of the dispersal changes from one direction to the other.

11 Under the *strongly asymmetric distance-dependent model*, the asymmetry is much stronger
 12 in the sense that the asymmetry factor d enters into the exponential decay of the col-
 13 onization rate. Asymmetry mirrors a weighting of the strength of colonization in one
 14 direction compared to the other, as well as an asymmetry in the average colonization
 15 distance. This creates a much stronger bias than in the previous case, as illustrated on
 16 Figure 1. More precisely, we have

$$f_+(k) = d^{\alpha k}/Z_+ \quad \forall k \geq 1 \quad \text{and} \quad f_-(k) = (1-d)^{\alpha k}/Z_- \quad \forall k \geq 1 \quad (17)$$

17 Now, the two normalization constants Z_+ and Z_- depend on d and are given respectively
 18 by

$$Z_+ = 1/(d(d^{-\alpha} - 1)) \quad \text{and} \quad Z_- = 1/((1-d)((1-d)^{-\alpha} - 1)) \quad (18)$$

19 in order to ensure again condition (8). This leads to the following matrix model:

$$m_{ij} = \begin{cases} d^{\alpha |i-j|}/Z_+ & \text{if } j > i \\ 0 & \text{if } i = j \\ (1-d)^{\alpha |i-j|}/Z_- & \text{if } i > j \end{cases} \quad (19)$$

1 Notice that in this case, the average colonization distances are

$$h_- = \frac{1}{\alpha \log(1/(1-d))} \quad , \text{ in the main direction of colonization} \quad (20)$$

2 and

$$h_+ = \frac{1}{\alpha \log(1/d)} \quad , \text{ in the opposite direction.} \quad (21)$$

3 Therefore, $h_- > h_+$ and the difference increases as d approaches zero.

4 *Grid stepping stone models.* We now consider models where the habitat patches are lo-
 5 cated on a regular two-dimensional grid. The asymmetry factor d has to be interpreted
 6 with some caution in this case, thus we will focus our attention on the simple situation
 7 where only the four nearest neighbors of a given habitat patch can be re-colonized (i.e.,
 8 assuming a von Neumann neighborhood of range 1). Thus, four directions of colonization
 9 are allowed: north, south, east and west. In this context, habitat patches are indexed
 10 by two numbers that indicate their positions, ik , so we index the matrix elements of
 11 M so that element $m_{ik,jl}$ characterizes the re-colonization probability from a patch at
 12 coordinate ik , to a patch at coordinate jl . As above, the asymmetry factor $d \in [0, 1/2]$
 13 may be interpreted as follows: $c(1-d)$ is the total colonization rate in the main direction
 14 of colonization and cd is the total colonization rate in the opposite direction. We con-
 15 sider then two forms of asymmetry; diagonal and horizontal. The first case characterizes
 16 a situation where an environmental gradient (such as wind, altitude, or ocean current)
 17 favors two directions of dispersal (in this case, south and west) equally with respect to
 18 the other two (north and east). The second case differs from the first in assuming that
 19 dispersal in two directions (south and north) is unaffected by the environmental gradient.

20 For the diagonal asymmetry, we assume that the main direction of the impact of asym-
 21 metry points toward the south-west, i.e. that the south and west directions of colonization
 22 are characterized by a colonization rate of $(1-d)/2$, and the north and east directions
 23 each have a colonization rate of $d/2$. The matrix M therefore reads

$$m_{ik,jl} = \begin{cases} d/2 & \text{if } j = i + 1, k = l \text{ or } j = i, l = k + 1 \\ (1-d)/2 & \text{if } i = j + 1, k = l \text{ or } j = i, k = l + 1 \\ 0 & \text{otherwise} \end{cases} \quad (22)$$

1 For the horizontal asymmetry, we assume that the main direction of colonization points
 2 toward the east; from a given habitat patch, colonization occurs to the west with a rate
 3 $d/2$, to the east with a rate $(1-d)/2$, while colonization in the north and south direction
 4 is unaffected by asymmetry and occurs at a rate $1/4$. Thus, the matrix M is given by

$$m_{ik,jl} = \begin{cases} d/2 & \text{if } j = i + 1, k = l \\ 1/4 & \text{if } i = j, |k - l| = 1 \\ (1-d)/2 & \text{if } i = j + 1, k = l \\ 0 & \text{otherwise} \end{cases} \quad (23)$$

5 We could consider other patterns of dispersal, but we will restrict our analysis to these
 6 two cases. They will allow us to differentiate the situation where only two (opposite)
 7 directions are affected by asymmetry from the situation where all directions are affected.

8 2.2.2. *Asymmetry in connectivity*

9 In our second set of analyses, we consider two types of global asymmetry in connectivity.
 10 The first case, called *circulating* asymmetry, allows only asymmetrically connected pairs
 11 of patches (colonization probability proportional to c from i to j and 0 from j to i). The
 12 second case, called *bidirectional* asymmetry, allows symmetric re-colonization between
 13 some fraction of the pairs of patches (colonization probability proportional to c in each
 14 direction). Starting from the so-called *cascade model* where all asymmetries point towards
 15 the same direction, we gradually reverse the direction of connections in a symmetric or
 16 asymmetric way. This procedure leads either to a circulating re-colonization pattern
 17 within the metapopulation, as observed for example in ocean systems, or mimics the
 18 pattern observed in river networks, where bidirectional movement is possible along some
 19 segments. We introduce the following parameters to characterize the asymmetry of the
 20 model: $T_C = \sum_{ij} m_{ij}$ denotes the total number of connections in the system, $T_S =$
 21 $\sum_{i>j} m_{ij} m_{ji}$ denotes the total number of symmetric (or bidirectional) connections and
 22 $L_D = \sum_{i>j} m_{ij}$ denotes the level of directionality, that is, the number of connections in
 23 the upper triangular part of the matrix M (i.e., in the direction opposite to the main
 24 direction of colonization).

25 We characterize the level of circulating asymmetry via the ratio $a_c = L_D/T_C$, which is

1 0 for the cascade model and increases to $1/2$ when asymmetric connections are randomly
 2 distributed. Here, we only consider values of $a_c < 1/2$; if $a_c > 1/2$, we can get identical
 3 results by setting the asymmetry parameter to $1 - a_c$ and reversing the orientation of the
 4 whole system. Bidirectional asymmetry is characterized via the parameter $a_b = T_S/T_C$,
 5 which is zero for the cascade model and can be as large as $1/2$ in the bidirectional model.
 6 In either case (circulating or bidirectional asymmetry), we start from the cascade model,
 7 either based on an island model ($m_{ij} = 1$ for $j < i$ and 0 otherwise: $T_C = n(n - 1)/2$),
 8 or on a two-dimensional grid model (pattern of connections as in (22), with $d = 1/2$:
 9 $T_C = 2(n - \sqrt{n})$). We then sample $f = a_c T_C$ (or $f = a_b T_C$) connections, without
 10 replacement, from these connections, and reassign them as follows.

11 *Circulating model*: keep the connections asymmetric but switch their direction:

$$\{m_{ij} = 1, m_{ji} = 0\} \rightarrow \{m_{ij} = 0, m_{ji} = 1\} \quad (24)$$

12 *Bidirectional model*: break the asymmetric connections and create bidirectional connec-
 13 tions elsewhere in the system, then sample f connections without replacement from the
 14 $(T_C - f)$ connections that were not chosen in the first sample and make them bidirectional:

$$\{m_{ij} = m_{kl} = 1, m_{ji} = m_{lk} = 0\} \rightarrow \{m_{ij} = m_{ji} = 0, m_{kl} = m_{lk} = 1\} \quad (25)$$

15 Figure 2 shows these two models.

16 Finally, we rescale the connectivity matrix so that the *average* per-patch connectivity
 17 is c (by dividing the binary connection matrix by the average number of neighbors,
 18 $n/2$ in the island case and 2 in the stepping-stone case). Asymmetry in connectivity is
 19 investigated only under the island and the stepping stone model. As in the distance-
 20 dependent model, connections have a weight that depends on their position and thus do
 21 not have conservative properties when permuted through the processes described above.

1 *2.3. Computing metapopulation capacity and extinction probability*

2 *2.3.1. Metapopulation capacity (λ_M)*

3 In the case where the matrix M is symmetric (i.e. when $d = 1/2$ and $f_+ = f_-$), it is
4 a direct consequence of the spectral theory of large Toeplitz matrices (Gray, 2006) that
5 λ_M approaches the largest row-sum of the matrix M for large system size, i.e. that

$$\lambda_M \simeq \sum_{k=1}^{n/2} f_+(k) + \sum_{k=1}^{n/2} f_-(k) \xrightarrow{n \rightarrow \infty} d + (1 - d) = 1 \quad (26)$$

6 Many methods are known in the mathematical literature for analyzing the largest eigen-
7 value (and more generally the whole spectrum) of large symmetric Toeplitz matrices (see
8 Gray (2006) for a detailed account on this subject). Nevertheless, no general method is
9 known for analyzing the largest eigenvalue of asymmetric Toeplitz matrices, which are
10 encountered here.

11 In the asymmetric dispersal strength case we can usually compute the metapopulation
12 capacity λ_M analytically, either for particular values of system size (n) or in the limit of
13 large system size. Indeed, when $d < 1/2$, the Perron-Frobenius theorem implies that λ_M
14 is non-negative and smaller than or equal to the largest row-sum of the matrix, i.e. smaller
15 than 1 for large system size. Furthermore, λ_M approaches 0 when d approaches 0. When
16 no analytical formula can be provided, we compute the largest eigenvalue λ_M numerically.

17 In the asymmetric connectivity case, there is no analytical expression for the largest
18 eigenvalue λ_M , so we estimate it by numerical simulation. Note also that in this situ-
19 ation, unlike in the asymmetric dispersal strength case, the irreducibility condition of
20 Ovaskainen and Hanski (2001) is not guaranteed, as random reconnections do not neces-
21 sarily create full connectivity in the network. This is particularly true when the number
22 of reconnections is small, as well as when the grid stepping stone model is considered. In
23 the latter case, we consider only real leading eigenvalues λ_M .

24 *2.3.2. Extinction probability (p_E)*

25 In order to contrast the theoretical results on metapopulation capacity obtained with
26 the deterministic model, we use numerical simulations to study the corresponding stochas-

1 tic model. The model is a Markovian stochastic model that describes the evolution of
2 habitat patch occupancy, using Monte Carlo simulation methods. We are interested in
3 the behavior of the extinction probability p_E of the whole system with respect to the
4 main parameters of the model, namely c , d and e . But now we consider a finite num-
5 ber of patches, $n = 100$, evolving according to the following stochastic process. At the
6 beginning, all patches are occupied. Each time step is divided into an extinction phase,
7 during which extinction occurs independently at each patch with probability e , and a
8 colonization phase, during which each empty patch i is recolonized with probability $c m_{ji}$
9 from patch j , given that this patch is occupied. We then evaluate the extinction proba-
10 bility p_E as the average proportion of empty habitat patches after $g = 1000$ generations.
11 We say that the system is stable if its survival probability is larger than 0. The average
12 is taken over $s = 1000$ independent simulations. Contrasting the relationship between
13 the time and the extinction probability in stochastic and deterministic metapopulation
14 models appears to be strongly sensitive to the way the process is truncated (Cairns and
15 Pollett, 2005). Indeed, if one were to let g grow arbitrarily large, while maintaining n
16 fixed, then the extinction probability would tend to 1, independently of the system pa-
17 rameters. On the contrary, letting g fixed while increasing n arbitrarily leads to a strictly
18 positive survival probability in all cases. The arbitrary values of the number of patches
19 n and the number of generation g considered here allow us to disentangle the impact of
20 various asymmetric patterns under similar conditions.

21 We consider four different models for the asymmetric dispersal strength case (the island
22 model, the strongly asymmetric distance-dependent model with $\alpha = 1$, the linear stepping
23 stone model and the grid stepping stone model with horizontal asymmetry) and four
24 different models for the asymmetric connectivity case (island and grid stepping stone
25 models with circulating and bidirectional asymmetry).

26 Ovaskainen and Hanski (2001) show that this system is well approximated by the system
27 given in (5). According to (6), the latter system is stable if and only if $\lambda_M(d) > e/c$.
28 Below, we explore the validity of this condition for the simulated system, in the context
29 of metapopulations with asymmetric dispersal strength.

3. Results

3.1. Metapopulation capacity λ_M

3.1.1. Asymmetry in dispersal strength

Figure 3a shows the behavior of the metapopulation capacity λ_M with respect to the asymmetry parameter d for the island model and for the stepping stone model. For the island model the slope of the curve is infinite at $d = 0$, and λ_M converges quickly to the value 1 as d approaches $1/2$ (i.e., the symmetric case). Remembering condition (6), this translates into a stabilization of the system, as soon as the colonization rate in the direction opposite to the main direction of colonization is greater than 0. Fitting a curve to the results in Figure 3a gives

$$\lambda_M(d) \approx (4d(1-d))^{0.3} \quad (27)$$

for large system size n .

Under the stepping stone model, the metapopulation capacity λ_M is shown to behave as

$$\lambda_M(d) \approx \sqrt{4d(1-d)} \quad (28)$$

for large system size n (this result is proved analytically in Appendix A.1). The results from this model are similar to those from the island model above (slope $+\infty$ in $d = 0$, rapid convergence to 1 as d approaches $1/2$), although the stability region where $\lambda_M(d) > e/c$ is smaller than in the previous case, as Figure 3a shows.

The value of λ_M remains relatively constant and displays the same value under both the island and the stepping stone model when d is above 0.36. However, below this value, the trajectories differentiate between the island and the stepping stone model. Following (6), viability is therefore predicted to decrease and to be the most affected by the asymmetry factor d under the stepping stone model. As expected, when the asymmetry is complete, both models predict extinction.

For the case of weak asymmetry and distance-dependent colonization (eq. 16), whether dispersal range is restricted ($\alpha = 10$) or not ($\alpha = 1$) (Figure 3b), the behavior of λ_M

1 resembles that of the stepping stone model in Figure 3a for large values of α (i.e. when
 2 the average colonization distance h is small). When α is small (i.e. when the average
 3 colonization distance h is large), the behavior of λ_M resembles that of the island model
 4 in Figure 3a. Small changes occur for λ_M when the asymmetry factor d is above 0.36.
 5 Similar to the results shown in Figure 3a, viability increases with dispersal ability.

6 Under strong asymmetry, viability quickly decreases with the asymmetry factor d
 7 (Fig. 1c). A decrease in dispersal ability buffers this effect for intermediate values of d .
 8 Interestingly, the shape of the relationship between d and λ_M differs from the previously
 9 studied cases (Fig. 3a and 3b) and depends on dispersal range α . When the asymmetry
 10 is strong (i.e. d is close to zero), the metapopulation capacity converges linearly to zero,
 11 at a rate increasing with a decrease in the dispersal range α . In the particular case where
 12 $\alpha = 1$, fitting a curve to the data points on Figure 3c gives

$$\lambda_M(d) \approx 2 \left(1 - \sqrt{1 - 3d(1 - d)} \right) \quad (29)$$

13 This result implies in particular that λ_M has *finite* slope in $d = 0$. More precisely, it
 14 follows from (29) that $\lambda'_M(0) = 3$. Appendix Appendix A.2 gives a proof that

$$\lambda'_M(0) \leq 3 \quad (30)$$

15 for all values of n (when $\alpha = 1$).

16 For other values of α , it can be inferred from Figure 3c that the slope of λ_M in $d = 0$
 17 also remains finite. This result therefore contrasts with the results obtained for the other
 18 models. Finally, Figure 3c shows that the size of the stability region delimited by the
 19 condition $\lambda_M(d) > e/c$ increases significantly with α under the present model.

20 When colonization takes place on a grid and the main direction of colonization is along
 21 a diagonal of the grid, the behavior of the metapopulation capacity λ_M differs little from
 22 the corresponding linear stepping stone model, as Figure 3d shows. This comes from the
 23 fact that the second dimension of the model does not enhance the survival probability of
 24 the metapopulation in this case. However, if only one direction displays an asymmetric
 25 pattern, i.e. the asymmetry is horizontal, then the metapopulation capacity is greatly
 26 enhanced, because of the possibility of persisting through re-colonizations in the direction
 27 *perpendicular* to the main direction of colonization. More precisely, the largest eigenvalue

1 of the matrix M is shown to behave for large system size as

$$\lambda_M^{2D}(d) \approx \frac{1 + \lambda_M^{1D}(d)}{2}, \quad (31)$$

2 where $\lambda_M^{1D}(d)$ is the metapopulation capacity under the linear stepping stone model, given
3 by (28). The result is illustrated on Figure 3d and proved in Appendix Appendix A.3.
4 As expected, when d tends to 0, $\lambda_M^{2D}(d)$ tends to 1/2 and not to 0, which arises from the
5 fact that the asymmetry affects only one direction. Even so, the slope of $\lambda_M^{2D}(d)$ is still
6 infinite in $d = 0$, as in the linear model.

7 Therefore, when two directions of colonization are affected by the asymmetry factor
8 d (Fig. 3d) and a grid stepping stone model of colonization is assumed, the shape of
9 the relationship between λ_M and d resembles that of the linear stepping stone model.
10 However, removing a direction where the asymmetry factor d applies qualitatively changes
11 the prediction of viability. The value of λ_M remains at relatively high values over the
12 range of d values and the stability region nearly doubles in size (Fig. 3d).

13 3.1.2. *Asymmetry in connectivity*

14 The metapopulation capacities λ_M obtained for different values of asymmetry in con-
15 nectivity, a_b and a_c , considering respectively a circulating and a bidirectional model, are
16 presented in Figure 4 for both the island model and the stepping stone model. For the
17 island model, the relationships between the metapopulation capacity and the asymme-
18 try in connectivity are nearly identical in the bidirectional and circulating cases and are
19 similar to the results from systems with asymmetry in the dispersal strength (Fig. 3). In
20 contrast, in the grid stepping stone model, the metapopulation capacity is highly variable,
21 even when the model is symmetric (a_b or $a_c = 1/2$). As the fraction of symmetric con-
22 nections decreases (from 1/2 to zero), the metapopulation capacity becomes even more
23 variable, and the patterns differ according to the type of asymmetry.

24 For the circulating model, the metapopulation capacity is strongly variable below an a_c
25 value of 0.25 (Fig. 4). This variability reflects the diversity of connectivity patterns that
26 can be generated by displacing connections. Indeed, changing the direction of connections
27 can lead to systems that are either stable or highly unstable. If this process generates
28 numerous habitat patches with only connections going out or going in (source and sink

1 habitat patches) the system is expected to be strongly prone to extinction. The presence
2 of source and sink habitat patches is reflected by the fact that the metapopulation capacity
3 remains below 1 over the range of a_c values considered.

4 For the bidirectional model, values of metapopulation capacity can be larger than 1
5 (Fig. 4). The process of creating bidirectional connections generates systems in which
6 connection density becomes strongly heterogeneous. This leads to the creation of iso-
7 lated habitats and strongly connected substructures weakly connected to each other.
8 Increasing the number of bi-directional connections quickly increases the metapopulation
9 capacity. However, the variability of the values obtained remains high, corresponding to
10 the diversity of the connectivity patterns obtained.

11 Finally, in both cases thresholds occur for the minimum metapopulation capacity, the
12 first at $\lambda_M = 1/2$. This phenomenon occurs because of the formation of cycles in the
13 graph through the reconnection process. Indeed, it can be checked that the largest
14 eigenvalue of a submatrix of M corresponding to a cycle in the graph is equal to $1/2$ (as the
15 adjacency matrix of a cycle is a circulating matrix and the non-zero coefficients of M are
16 all equal to $1/2$ in the grid stepping stone model). In the circulating model, these cycles
17 appear only after a significant amount of link-flipping ($a_c > 0.2$ in the present sample),
18 whereas they appear for any $a_b > 0$ in the bidirectional model (as a cycle of length 2 is
19 automatically created after one reconnection in this case). One observes the formation
20 of further thresholds for the bidirectional model, corresponding to the appearance of
21 new structures in the graph (e.g., the next threshold is at $\lambda_M = 1/\sqrt{2} \approx 0.707$, which
22 corresponds to the formation of adjacent cycles of length 2).

23 3.2. Extinction probability p_E versus λ_M

24 3.2.1. Asymmetry in dispersal strength

25 The results are illustrated in Figure 5, where both the metapopulation capacity λ_M
26 and the extinction probability p_E are represented as functions of the asymmetry factor d ,
27 for various values of the colonization rate c (the local extinction rate e is kept constant
28 at 0.1, as only the ratio e/c matters in (6)). Four different models are considered: the

1 island model (Fig. 5a), the strongly asymmetric distance-dependent model with $\alpha = 1$
2 (Fig. 5b), the linear stepping stone model (Fig. 5c) and the grid stepping stone model
3 with horizontal asymmetry (Fig. 5d).

4 Under the island model, Figure 3a suggests that for the parameters considered, the
5 metapopulation can persist (the extinction probability predicted from the metapopu-
6 lation capacity drops below 1) as soon as d increases slightly above zero. This result
7 matches the numerical results shown in Figure 5; for the parameters considered, the ex-
8 tinction probability drops rapidly below 1 as d increases from 0. Differences in extinction
9 probability obtained with the three models of colonization along the range of values of d
10 are relatively constant. Their behavior is relatively similar; they quickly level off to e/c ,
11 the value predicted for a symmetric metapopulation (6). Those results are reflected by
12 the behavior of the metapopulation capacity λ_M : it stays close to 1 for a wide range of
13 values of d (from to $d = 0.5$) before finally dropping to 0 when d reaches 0.

14 Under the strongly asymmetric distance-dependent model, assuming large dispersal
15 ability ($\alpha = 1$) (Fig. 5b), the extinction probability stays equal to 1 for a large range
16 of d values. The extinction probability reaches a threshold value at quite high values
17 of d , which depend on value of c considered. The transition from maximal to minimal
18 extinction probabilities is more gradual than in the previous case (Fig. 5a).

19 Under the stepping stone model (Fig. 5c), a similar phenomenon occurs: the extinction
20 probability slowly decreases with increasing symmetry, but the decrease starts immedi-
21 ately when d is slightly larger than 0. On the other hand, the threshold values reached
22 for $d = 1/2$ are higher in this case. This is explained by the inherent low connectivity
23 of the stepping stone model, whose extinction probability is therefore larger than that of
24 other models. The parameter range over which extinction decreases increases as (e/c) in-
25 creases. Under this model, the predictions of extinction according to the metapopulation
26 capacity λ_M disagree with the simulation results.

27 Finally, the behavior of the extinction probability is illustrated for the grid stepping
28 stone model with horizontal asymmetry (Fig. 5d). Similar to the results for the island
29 model (Fig. 5a), a quick decrease of the extinction probability when d is slightly larger
30 than zero is predicted. Expected extinction probabilities (e/c) are reached for relatively
31 low values of d and converge more rapidly when colonization is high.

1 3.2.2. *Asymmetry in connectivity*

2 In the island model, extinction probability reaches 1 under both the bidirectional and
3 the circulating models, for all values of colonization rates, as the system becomes com-
4 pletely asymmetric (Figure 6). As asymmetry in connectivity decreases, the extinction
5 probability drops extremely rapidly when $c \geq 0.3$; when $c = 0.2$ it drops for a_b or $a_c > 0.1$,
6 and for $c = 0.1$ the metapopulation never persists.

7 Overall, persistence is very low in the grid stepping stone model and the behavior of
8 the metapopulation capacity over the range of asymmetric values a_b and a_c differentiates
9 between the bidirectional and circulating models. The extinction probability decreases
10 faster with increased a_b than with increased a_c (Figure 6). For a given level of asymme-
11 try, the values of the colonization rate c required for metapopulation viability are higher
12 for the circulating case than for the bidirectional case. Under the circulating model, the
13 proportion of permuted connections, a_c , needed to provide a viable network of habitat
14 patches is high (30–50%); whatever colonization rate is considered, all the connections
15 have to be shuffled in order to reach the lowest extinction probability. Under the bidirec-
16 tional model, a surprisingly low proportion of bidirectional connections, a_b , (15-20 %) is
17 sufficient to drastically reduce the extinction probability of the metapopulation (Figure
18 6). Extinction rapidly declines as the number of symmetric connections increases. When
19 the number of reversed connections reaches 40%, the extinction probability stabilizes
20 at a low value. These results might be predicted from the considerably lower average
21 metapopulation capacities in the circulating case. However, because the connection ma-
22 trices are not irreducible in this case, it is unclear whether the metapopulation capacity
23 can be interpreted in the same way. Indeed, for a given level of asymmetry a_b the mean
24 metapopulation capacities are higher in the grid stepping stone model than in the is-
25 land model, but the extinction probabilities are also higher, indicating that the standard
26 comparisons based on metapopulation capacities do break down in this case.

1 4. Discussion

2 4.1. Asymmetry in dispersal strength

3 Overall, persistence is relatively well maintained when asymmetry in dispersal strength
4 is less than 25%. Below this level of asymmetry, extinction probabilities resembles those
5 from a completely symmetric system. Above this value, extinction predictions are highly
6 sensitive to the migration model assumed and to the shape of asymmetry in the dispersal
7 pattern. When a bias in re-colonization direction exceeds 35%, viability predictions
8 quickly drop under both the stepping stone model and the distance-dependent model
9 of migration. The worst situation for species viability is a pattern of re-colonization in
10 which both direction and range of re-colonization are biased in one direction, under a
11 distance-dependent migration model, when the species has a large dispersal ability ($\alpha =$
12 1) (Figure 5b). Indeed, under those conditions, a small bias in the colonization pattern
13 has the strongest impact on viability predictions, while for other models, the impact
14 remains weak. Ultimately, when no limitation in distance is considered (island model) or
15 when re-colonization is symmetric in some direction (such as e.g. for the stepping stone
16 with horizontal asymmetry) viability predictions remain stable until asymmetry becomes
17 extreme (more than 80% of re-colonization bias in one direction).

18 Interestingly, the two patterns of re-colonization that provide the lowest extinction
19 probability appear to be common in ecosystems subject to environmental gradient. For
20 example, in dynamic marine environments, where advection by currents carries individ-
21 uals far from natal populations (Caley et al., 1996), such dynamics might provide a high
22 re-colonization potential between distant populations. Such patterns appear to be fre-
23 quently associated with a local strong connectivity. Several recent studies have showed
24 strong evidence that individuals can remain close to their natal habitats by exploiting
25 local circulation patterns (Swearer et al., 2002; Warner and Cowen, 2002; Cowen et al.,
26 2006; Becker et al., 2007; Cowen and Sponaugle, 2009; Morgan et al., 2009). In particular,
27 Morgan et al. (2009) demonstrate that in conditions of wind-driven offshore transport
28 and strong upwelling regions, marine larvae are more likely to recruit close to natal popu-
29 lations than previously thought. Although dispersal ability certainly affects the viability

1 of metapopulations, dispersal pattern that allows either some local symmetry or/and long
2 distance dispersal might simply be an evolution in heterogeneous environment to avoid
3 extinction.

4 *4.2. Asymmetry in connectivity*

5 For asymmetry in connectivity, when dispersal distance is unlimited (the island model),
6 viability does not differ between the two main patterns investigated. A small proportion
7 of reverse connections quickly lead to viability, because the matrix has high connectance
8 and because the initial configuration (before permutation of connections) follows a cas-
9 cade model. Even though a pure cascade model is unviable, it provides a structure that
10 allows full connectivity between all habitat patches. Under an island model, gradually
11 permuting connections leads to a situation where re-colonization is allowed through the
12 entire system. However, when re-colonization is limited in distance (as in the grid step-
13 ping stone model) and the number of connections is reduced, viability is much harder to
14 achieve. To generate a configuration in which re-colonization process is possible across
15 the entire network, the number of connection permutations must be fairly high. However,
16 this global connectivity is achieved faster in the bi-directional model than in the circu-
17 lating model. Even with a high colonization rate, a very small proportion of asymmetry
18 in connectivity quickly increases the extinction probability under the circulating model,
19 while under the bidirectional model, extinction predictions remain similar to those ex-
20 pected under symmetry when 10-20% of asymmetry is considered (i.e., when a_b decreases
21 to $\approx 0.3 - 0.5$). In the circulating model, the permutation process gradually creates large
22 networks of habitat patches which increase the average length of successive connections
23 to allow re-colonization, while the bidirectional model reinforces the local re-colonization
24 potential of sub-networks of habitat patches. The resulting local sub-structure provides
25 sources of colonizers for the habitats that might be more prone to extinction.

26 Our results agree with those of Vuilleumier and Possingham (2006). They contrast the
27 prediction of metapopulation extinction under a symmetric (only bidirectional connec-
28 tions) and asymmetric (only one-directional connections) connectivity matrix, given any
29 random number of connections. They show that the viability under asymmetric coloniza-

1 tion pattern is much lower than under a symmetric one. Our approach refines their study
2 and differs in four aspects: the starting condition is a cascade model, intermediate forms
3 of asymmetry are considered (a_b factor), specific numbers of connections are considered
4 (grid stepping stone vs island model) and the generation of the connectivity matrix is
5 performed under strong constraints which allow the creation of large loops or strong local
6 connectivity in the system.

7 The connectivity matrices generated here are neither precisely one-dimensional nor two-
8 dimensional and share some properties of dendritic networks (Tarboton, 1996; Campbell
9 Grant et al., 2007). Some authors have shown that such structures affect metapopula-
10 tion dynamics, inducing source-sink dynamics (Hanfling and Weetmann, 2006; Labonne
11 et al., 2008) and affecting the patterns of community diversity (Economio and Keitt,
12 2008; Rodriguez-Iturbe et al., 2009) as well as genetic relatedness (Wofford et al., 2005;
13 Labonne et al., 2008), diversity (Jansson et al., 2005; Morrissey and Kerckhove, 2009),
14 and species range distribution (Gaylord and Gaines, 2000; Leyer, 2006; Gurnell et al.,
15 2008). Such networks are a longstanding object of study for hydrologists (e.g. Horton
16 1945), who differentiate river networks that are structured in a few poorly interconnected
17 groups of patches (Hortonian) from networks that have a better balance between local
18 and long-distance connectivity (non-Hortonian). In this context, Labonne et al. (2008)
19 showed that in Hortonian networks, extinction probability is enhanced, as root patches
20 often go extinct, splitting the metapopulation into disconnected components with shorter
21 persistence times. Speirs and Gurney (2001) and Lutscher et al. (2005) demonstrate that
22 this effect is enhanced when dendritic structures are associated with a directional bias
23 of re-colonization. Our bidirectional and circulating asymmetry cases are similar to non-
24 Hortonian and Hortonian networks, but we allow for a large range of spatial configurations
25 in which local and global clustering is allowed. We also confirm that this effect strongly
26 depends on the ability of the species to disperse: when long dispersal is allowed, as in
27 the island model, there is little difference in extinction probability among the networks
28 considered.

1 4.3. Predicted and actual threshold values for extinction

2 Predicted and actual threshold values in asymmetry in dispersal strength show a clear
3 correspondence between the predicted threshold value d^* computed from the equation
4 $\lambda_M(d^*) = e/c$ and the value for which the probability p_E drops below the value 1 when
5 the island model and the two stepping stone models are considered. However, a careful
6 observation of the results shows that, for the distance-dependent model, the predicted
7 threshold value d^* computed from the equation $\lambda_M(d^*) = e/c$ does not occur exactly
8 where the probability p_E drops below the value 1 (Figure 3b). The observed discrepancies
9 can be explained in various ways.

10 First of all, the predicted threshold value d^* is computed in the framework of the
11 model (5), a *deterministic* model which does not *a priori* fully match with our *stochastic*
12 simulations of the actual extinction probability.

13 We also expect differences because of differences in the underlying assumptions of the
14 models. The deterministic and stochastic models considered here would lead to identical
15 predictions only for a large number of habitat patches that are equally connected to
16 other habitat patches. Looking at a system where re-colonization from an habitat patch
17 is restricted to a small number of habitat patches (such as the stepping-stone model)
18 violates such an assumption and leads to deviations from the stochastic system. In
19 addition, boundary effects cannot be neglected in a system with a relatively small number
20 of patches.

21 Moreover, the stochastic model is evaluated at quasi-stationary equilibrium (that is,
22 after a given number of generations). As shown by Cairns and Pollett (2005), the rela-
23 tionship between the time and the extinction probability in stochastic and deterministic
24 metapopulation models can be strongly sensitive to the way the process is truncated.
25 As the number of generations increases, so do the extinction probability and this inde-
26 pendently of the system parameters. Similarly, extinction probability in the stochastic
27 model decreases with the size of the system. Part of the discrepancies observed between
28 the stochastic and deterministic predictions is expected from the chosen metapopulation
29 size and cut-off used. A detailed analysis of the impact of these parameters for each of
30 the model investigated here could have been of interest but goes beyond the purpose of

1 this study.

2 Finally, as mentioned above, the the asymmetric connectivity model does not guarantee
3 irreducibility of the landscape matrix M . When M is reducible, the metapopulation is
4 divided into groups of patches which are disconnected from each other and the condition
5 $\lambda_M \geq e/c$ established by Hanski and Ovaskainen (2001) is not applicable. There is still
6 much to say about the profile of surviving metapopulations (that is, the probability of
7 persistence of a patch given its position). Given the theoretical result of Ovaskainen and
8 Hanski (2001), it is known that when the recolonization matrix M is irreducible, the
9 limit profile vector p^* is positive everywhere. Lutscher et al. (2007) refine this picture
10 and show that in environment with unidirectional flow there is an upstream limit above
11 which a patch survival probability is close to zero, while a linear and strictly positive
12 profile seems to emerge below this limit. Studying further this profile under our model
13 is a promising future research track.

14 *4.4. Robustness of our model*

15 Our stochastic simulations are performed in discrete time: at each time step, we let all
16 the extinctions occur first, and then simulate the colonizations. Reversing the order of
17 events does not modify the behavior of the system during simulations, as we start with the
18 situation where all habitat patches are occupied. However, if persistence is evaluated after
19 the extinction events instead of the colonization events, viability predictions are lower,
20 as shown on Figure 7. Nevertheless, the general behavior of the extinction probability in
21 relationship to asymmetry is not affected.

22 Continuous- and discrete-time colonization-extinction models of metapopulations can
23 also differ in their predictions of extinction (Frank, 2005). In continuous-time models,
24 extinctions and colonizations are not ordered. Extinctions occur at rate e , while col-
25 onizations between habitat patches i and j occur at rate $c m_{ij}$, and the time intervals
26 between these events are assumed to be independent and exponentially distributed. As
27 Figure 8 shows, our results are robust to this change of model: simulations performed
28 in discrete time or continuous time lead to similar behavior of the extinction probability
29 with respect to the asymmetry factor d .

1 **5. Conclusion**

2 In heterogeneous environments, populations are fragmented and form metapopulations
3 which persist through processes of extinction and re-colonization. Due to environmental
4 heterogeneity, those fragmented populations form complex networks of habitat patches
5 that can display asymmetry in dispersal. Such networks have dynamic, ecological and
6 genetic properties that strongly differ from those observed in homogeneous systems and
7 suffer from a general lack of theoretical exploration (Vuilleumier and Possingham, 2006;
8 Campbell Grant et al., 2007; Labonne et al., 2008; Morrissey and Kerckhove, 2009).
9 Given fixed values of standard metapopulation parameters such as overall colonization
10 rate, extinction rate, and connectivity, we explored how the level and pattern of re-
11 colonization asymmetry affect the metapopulation capacity and persistence.

12 We found that a directional bias in dispersal strength smaller than 25% does not affect
13 metapopulation persistence; this threshold value reaches 80% when metapopulation bene-
14 fits from a strong general connectivity (the island model) or with strong local connectivity
15 (local horizontal symmetry). However, when the connectivity is generally weak (stepping
16 stone model), a bias of as little as 35% drastically reduces viability. This effect is even
17 stronger when the re-colonization bias affects both the strength and the average distance
18 of dispersal. Networks that allow for a balance between local and global (long-distance)
19 connectivity provide higher persistence than networks that allow for global connectivity
20 and large circulating re-colonization patterns (island model).

21 **Acknowledgments**

22 We thank I.L. Chatterji for inspiring discussions. SV and BMB thank the Mathemat-
23 ical Biosciences Institute for hospitality during the period during which this work was
24 initiated. This work was supported by the grant PZ00P3-121702 to SV from the Swiss
25 National Science Foundation and US National Science Foundation IGERT grant DGE-
26 0801544 (BMB). The authors acknowledge the University of Florida High-Performance
27 Computing Center (URL: <http://hpc.ufl.edu>) for providing computational resources and
28 support that have contributed to the research results reported within this paper.

1 **References**

- 2 Amarasekare, P., 2004. The role of density-dependent dispersal in source-sink dynamics.
3 *J. Theor. Biol.* 226, 159-168.
- 4 Bay, L. K., Caley, M. J. M., Crozier, R. H., 2008. Meta-population structure in a coral
5 reef fish demonstrated by genetic data on patterns of migration, extinction and re-
6 colonisation. *BMC Evol. Biol.* 8, 248.
- 7 Becker, B. J., Levin, L. A., Fodrie, F. J., McMillan, P. A., 2007. Complex larval connec-
8 tivity patterns among marine invertebrate populations. *Proc. Natl. Acad. Sci. U. S.*
9 *A.* 104, 3267-3272.
- 10 Benda, L., Poff, N. L., Miller, D., Dunne, T., Reeves, G., Pess, G., Pollock, M., 2004.
11 The network dynamics hypothesis: How channel networks structure riverine habitats.
12 *Bioscience.* 54, 413-427.
- 13 Bode, M., Bode, L., Armsworth, P. R., 2006. Larval dispersal reveals regional sources
14 and sinks in the Great Barrier Reef. *Mar Ecol Prog Ser.* 308, 17-25.
- 15 Bolnick, D. I., Caldera, E. J., Matthews, B., 2008. Evidence for asymmetric migration
16 load in a pair of ecologically divergent stickleback populations. *Biol. J. Linn. Soc.* 94,
17 273-287.
- 18 Cairns, B. J., Pollett, F., 2005. Approximating persistence in a general class of population
19 processes. *Theor. Popul. Biol.* 68, 77-90.
- 20 Caley, M. J., Carr, M. H., Hixon, M. A., Hughes, T. P., Jones, G. P., Menge, B. A., 1996.
21 Recruitment and the local dynamics of open marine populations. *Annu. Rev. Ecol.*
22 *Syst.* 27, 477-500.
- 23 Campbell Grant, E. H., Lowe, W. H., Fagan, W. F., 2007. Living in the branches:
24 population dynamics and ecological processes in dendritic networks. *Ecol. Lett.* 10,
25 165-175.
- 26 Chaput-Bardy, A., Fleurant, C., Lemaire, C., Secondi, J., 2009. Modelling the effect of
27 in-stream and overland dispersal on gene flow in river networks. *Ecol. Modelling.* 220,
28 3589-3598.
- 29 Cheal, A. J., Delean S., Sweatman, H., Thompson, A. A., 2007. Spatial synchrony in
30 coral reef fish populations and the influence of climate. *Ecology.* 88, 158-169.

- 1 Cowen, R. K., Paris, C. B., Srinivasan, A., 2006. Scaling of connectivity in marine
2 populations. *Science*. 311, 522-527.
- 3 Cowen, R. K., Sponaugle, S., 2009. Larval Dispersal and Marine Population Connectivity.
4 *Annu. Rev. Mar. Sci.* 1, 443-466.
- 5 Durrett, R., Levin, S., 1994. The importance of being discrete (and spatial). *Theor.*
6 *Popul. Biol.* 46, 363-394.
- 7 Economo, E. P., Keitt, T. H., 2008. Species diversity in neutral metacommunities: a
8 network approach. *Ecol. Lett.* 11, 52-62.
- 9 Fagan, W. F., 2002. Connectivity, fragmentation, and extinction risk in dendritic metapop-
10 ulations. *Ecology*. 83, 3243-3249.
- 11 Finn, D. S., Theobald, D. M., Black, W. C., Poff, N. L., 2006. Spatial population genetic
12 structure and limited dispersal in a Rocky Mountain alpine stream insect. *Mol. Ecol.*
13 15, 3553-3566.
- 14 Fortuna, M. A., Gomez-Rodriguez, C., Bascompte, J., 2006. Spatial network structure
15 and amphibian persistence in stochastic environments. *Proc. R. Soc. London, Ser. B.*
16 273, 1429-1434.
- 17 Frank, K., 2005. Metapopulation persistence in heterogeneous landscapes: Lessons about
18 the effect of stochasticity. *Am. Nat.* 165, 374-388.
- 19 Friedman, J., Stein, Z., 1980. Influence of seed-dispersal mechanisms on the dispersion
20 of *Anastatica hierochuntica* (Cruciferae) in the Negev desert, Israel. *J. Ecol.* 68, 43-50.
- 21 Gaines, S. D., Gaylord, B. Largier, J. L., 2003. Avoiding current oversights in marine
22 reserve design. *Ecol. Appl.* 13, S32-S46.
- 23 Gaylord, B., Gaines, S. D., 2000. Temperature or transport? Range limits in marine
24 species mediated solely by flow. *Am. Nat.* 155, 769-789.
- 25 Gurnell, A., Thompson, K., Goodson, J., Moggridge, H., 2008. Propagule deposition
26 along river margins: linking hydrology and ecology. *J. Ecol.* 96, 553-565.
- 27 Gornall, R. J., Hollingsworth, P. M., Preston, C. D., 1998. Evidence for spatial structure
28 and directional gene flow in a population of an aquatic plant, *Potamogeton coloratus*.
29 *Heredity* 80, 414-421.
- 30 Gray R. M., 2006. Toeplitz and Circulant Matrices: A Review. *FnTCIT* .2(3), 155-239.
- 31 Hanski, I., 1999, *Metapopulation ecology*: Oxford University Press. Oxford University.

- 1 Hanski, I., Gyllenberg, M., 1997. Uniting two general patterns in the distribution of
2 species. *Science*. 275, 397-400.
- 3 Hanfling, B., Weetman, D., 2006. Concordant genetic estimators of migration reveal an-
4 thropogenically enhanced source-sink population structure in the River Sculpin, *Cottus*
5 *gobio*. *Genetics*. 173, 1487-1501.
- 6 Holt, R. D., 1996. Adaptive evolution in source-sink environments: Direct and indirect
7 effects of density-dependence on niche evolution. *Oikos*. 75, 182-192.
- 8 Horton, R.E., 1945. Erosional development of streams and their drainage basins: hy-
9 drophysical approach to quantitative morphology. *Geol. Soc. Am. Bull.* 56, 275-370.
- 10 Hughes, J. M., Schmidt, D. J., Finn, D. S., 2009. Genes in Streams: Using DNA to
11 Understand the Movement of Freshwater Fauna and Their Riverine Habitat. *Bioscience*.
12 59, 573-583.
- 13 Imbert, E., Lefevre, F., 2003. Dispersal and gene flow of *Populus nigra* (Salicaceae) along
14 a dynamic river system. *J. Ecol.* 91, 447-456.
- 15 James, M. K., Armsworth, P. R., Mason, L. B., Bode, L., 2002. The structure of reef
16 fish metapopulations: modelling larval dispersal and retention patterns. *Proc. R. Soc.*
17 *London, Ser. B.* 269, 2079-2086.
- 18 Jansson, R., Zinko, U., Merritt, D. M., Nilsson, C., 2005. Hydrochory increases riparian
19 plant species richness: a comparison between a free-flowing and a regulated river. *J.*
20 *Ecol.* 93, 1094-1103.
- 21 Kawecki, T. J., 1995. Demography of Source-Sink Populations and the Evolution of
22 Ecological Niches. *Evol. Ecol.* 9, 38-44.
- 23 Kawecki, T. J., Holt, R. D., 2002. Evolutionary consequences of asymmetric dispersal
24 rates. *Am. Nat.* 160, 333-347.
- 25 Kawecki, T. J., Stearns, S. C., 1993. The Evolution of Life Histories in Spatially Hetero-
26 geneous Environments: Optimal Reaction Norms Revisited. *Evol. Ecol.* 7, 155-174.
- 27 Keddy, P. A., 1981. Experimental demography of the sand-dune annual, *Cakile edentula*,
28 growing along an environmental gradient in Nova Scotia. *J. Ecol.* 69, 615-630.
- 29 Kimura, M., Weiss, G. H., 1964. The stepping stone model of population structure the
30 the decrease of genetic correlation with distance. *Genetics*. 49, 561-576.
- 31 Labonne, J., Ravigne, V., Parisi, B., Gaucherel, C., 2008. Linking dendritic network

1 structures to population demogenetics: The downside of connectivity. *Oikos*. 117,
2 1479-1490.

3 Largier, J. L., 2003. Considerations in estimating larval dispersal distances from oceano-
4 graphic data. *Ecol. Appl.* 13, S71-S89.

5 Levin, L. A., 2006. Recent progress in understanding larval dispersal: new directions and
6 digressions. *Integr. Comp. Biol.* 46, 282-297.

7 Levins, R., 1969 Some demographic and genetic consequences of environmental hetero-
8 geneity for biological control. *Bull. Entomol. Soc. Amer.* 15, 237-240.

9 Levins, R., 1970. Extinction. *Lect. Notes Math.* 2, 75-107.

10 Leyer, I., 2006. Dispersal, diversity and distribution patterns in pioneer vegetation: The
11 role of river-floodplain connectivity. *J. Veg. Sci.* 17, 407-416.

12 Lutscher, F., Pachevsky, E., Lewis, M. A., 2005. The effect of dispersal patterns on
13 stream populations. *Siam J. Ap. Math.* 65, 1305-1327.

14 Lutscher, F., McCauley, E., Lewis, M. A., 2007. Spatial patterns and coexistence mech-
15 anisms in systems with unidirectional flow. *Theor. Popul. Biol.* 71, 267-277.

16 Morgan, S. G., Fisher, J. L., Miller, S. H., McAfee, S. T., Largier, J. L., 2009. Nearshore
17 larval retention in a region of strong upwelling and recruitment limitation. *Ecology*.
18 90, 3489-3502.

19 Morris, D. W., 1991. On the Evolutionary Stability of Dispersal to Sink Habitats. *Am.*
20 *Nat.*137, 907-911.

21 Morrissey, M. B., de Kerckhove, D. T., 2009. The Maintenance of Genetic Variation Due
22 to Asymmetric Gene Flow in Dendritic Metapopulations. *Am. Nat.*174, 875-889.

23 Muneeppeerakul, R., Bertuzzo, E., Rinaldo, A., Rodriguez-Iturbe, I., 2008. Patterns of
24 vegetation biodiversity: The roles of dispersal directionality and river network structure.
25 *J Theor. Biol.* 252, 221-229.

26 Ovaskainen, O. 2003., Habitat destruction, habitat restoration and eigenvector-eigenvalue
27 relations. *Math. Biosci.* 181, 165-176.

28 Ovaskainen, O., Hanski, I., 2001. Spatially structured metapopulation models: Global
29 and local assessment of metapopulation capacity. *Theor. Popul. Biol.* 60, 281-302.

30 Pulliam, H. R., 1988. Sources, sinks, and population regulation. *Am. Nat.* 132, 652-661.

31 Pulliam, H. R., Danielson, B. J., 1991. Sources, sinks, and habitat selection - a landscape

1 perspective on population dynamics. *Am. Nat.* 137, S50-S66.

2 Rodriguez-Iturbe, I., Muneeppeerakul, R., Bertuzzo, E., Levin, S. A., Rinaldo A., 2009.

3 River networks as ecological corridors: A complex systems perspective for integrating

4 hydrologic, geomorphologic, and ecologic dynamics. *Water Resour. Res.*45, W01413.

5 Saether, B. E., Engen, S., Lande, R., 1999. Finite metapopulation models with density-

6 dependent migration and stochastic local dynamics *Proc. R. Soc. London, Ser. B.* 266,

7 113-118.

8 Schooley, R. L., Wiens, J. A., 2003. Finding habitat patches and directional connectivity.

9 *Oikos.* 102, 559-570.

10 Speirs, D. C., Gurney, W. S. C., 2001. Population persistence in rivers and estuaries.

11 *Ecology.* 82, 1219-1237.

12 Swearer, S. E., Shima, J. S., Hellberg, M. E., Thorrold, S. R., Jones, G. P., Robertson,

13 D. R., Morgan S. G. et al., 2002. Evidence of self-recruitment in demersal marine

14 populations. *Bull. Mar. Sci.* 70, 251-271.

15 Tarboton, D. G., 1996. Fractal river networks, Horton's laws and Tokunaga cyclicity. *J*

16 *Hydrol.* 187, 105-117.

17 Thorrold, S. R., 2006. Ocean ecology: Don't fence me in. *Curr. Biol.* 16, R638-R640.

18 Vuilleumier, S., Possingham, H. P., 2006. Does colonization asymmetry matter in metapop-

19 ulations? *Proc. R. Soc. London, Ser. B.* 273, 1637-1642.

20 Warner, R. R., Cowen, R. K., 2002. Local retention of production in marine populations:

21 Evidence, mechanisms, and consequences. *Bull. Mar. Sci.* 70, 245-249.

22 Watkinson, A. R., 1985. On the abundance of plants along an environmental gradient.

23 *J. Ecol.* 73, 569-578.

24 Wofford, J. E. B., Gresswell, R. E., Banks, M. A., 2005. Influence of barriers to movement

25 on within-watershed genetic variation of coastal cutthroat trout. *Ecol. Appl.* 15, 628-

26 637.

27 Young, C. R., Fujio, S., Vrijenhoek, R. C., 2008. Directional dispersal between mid-

28 ocean ridges: deep-ocean circulation and gene flow in *Ridgeia piscesae*. *Mol. Ecol.* 17,

29 1718-1731.

1 6. Figures

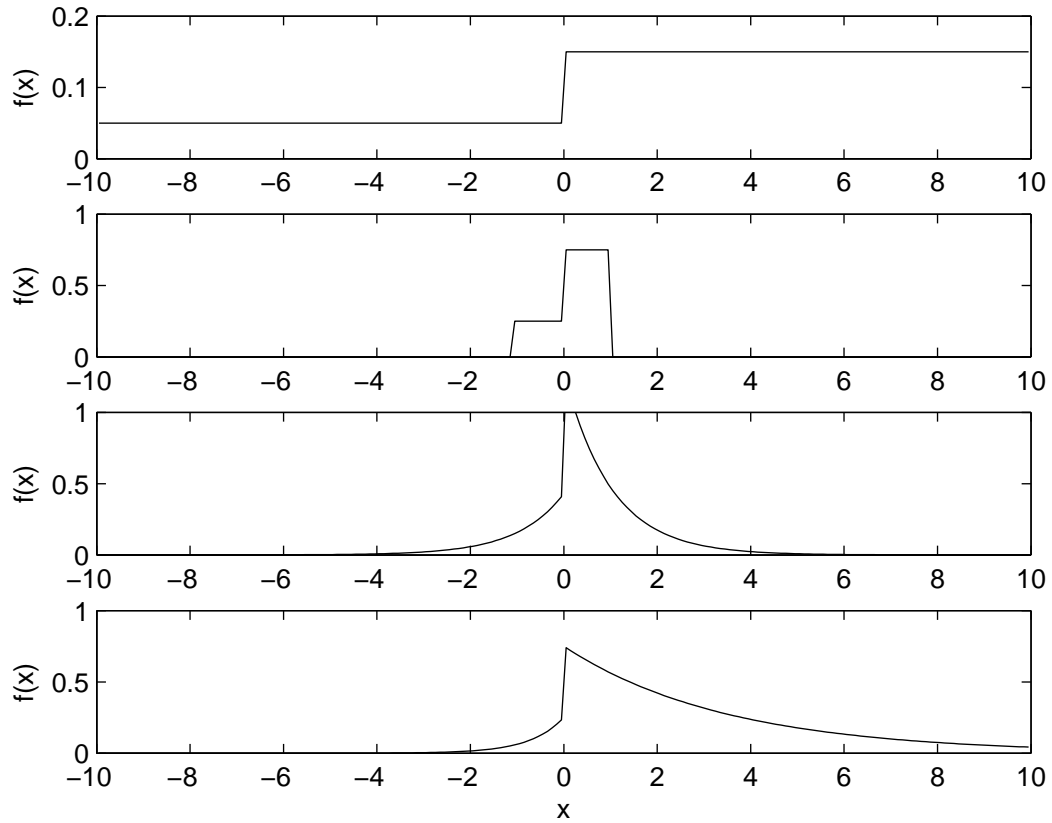


Figure 1: Decay of the colonization rate $f(x)$ with the distance x from the focal habitat patch in (from top to bottom): the island model, the stepping stone model, the weakly and strongly asymmetric distance-dependent models. Here, the asymmetry factor $d = 1/4$ (and $\alpha = 1$ in the distance-dependent models).

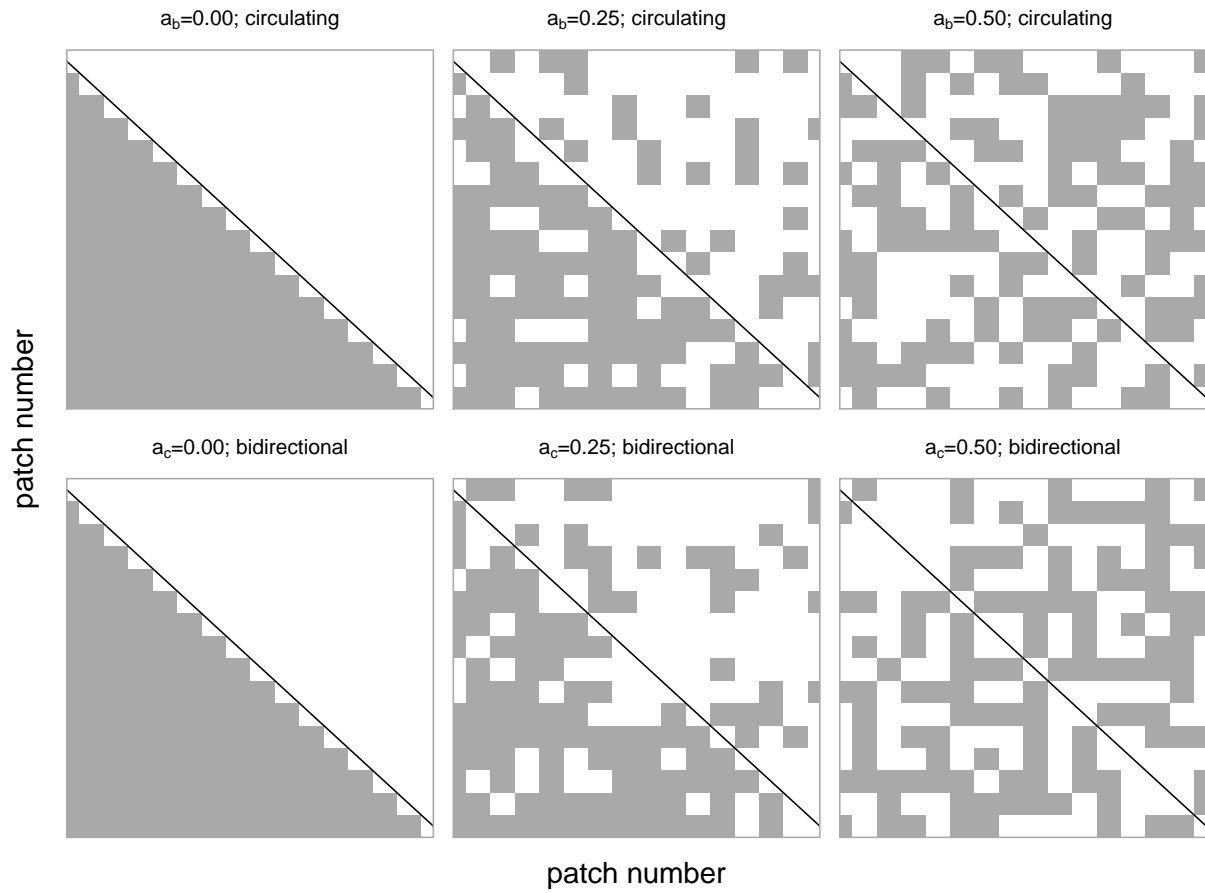


Figure 2: Patterns of asymmetry in colonization. Connection matrices for island model, 16×16 system. Top row, circulating: for $a_c = 1/2$ (top right), the system is antisymmetric ($m_{ij} = 1 - m_{ji}$ for all i, j). Bottom row, bidirectional: for $a_b = 1/2$ (bottom right), the system is symmetric.

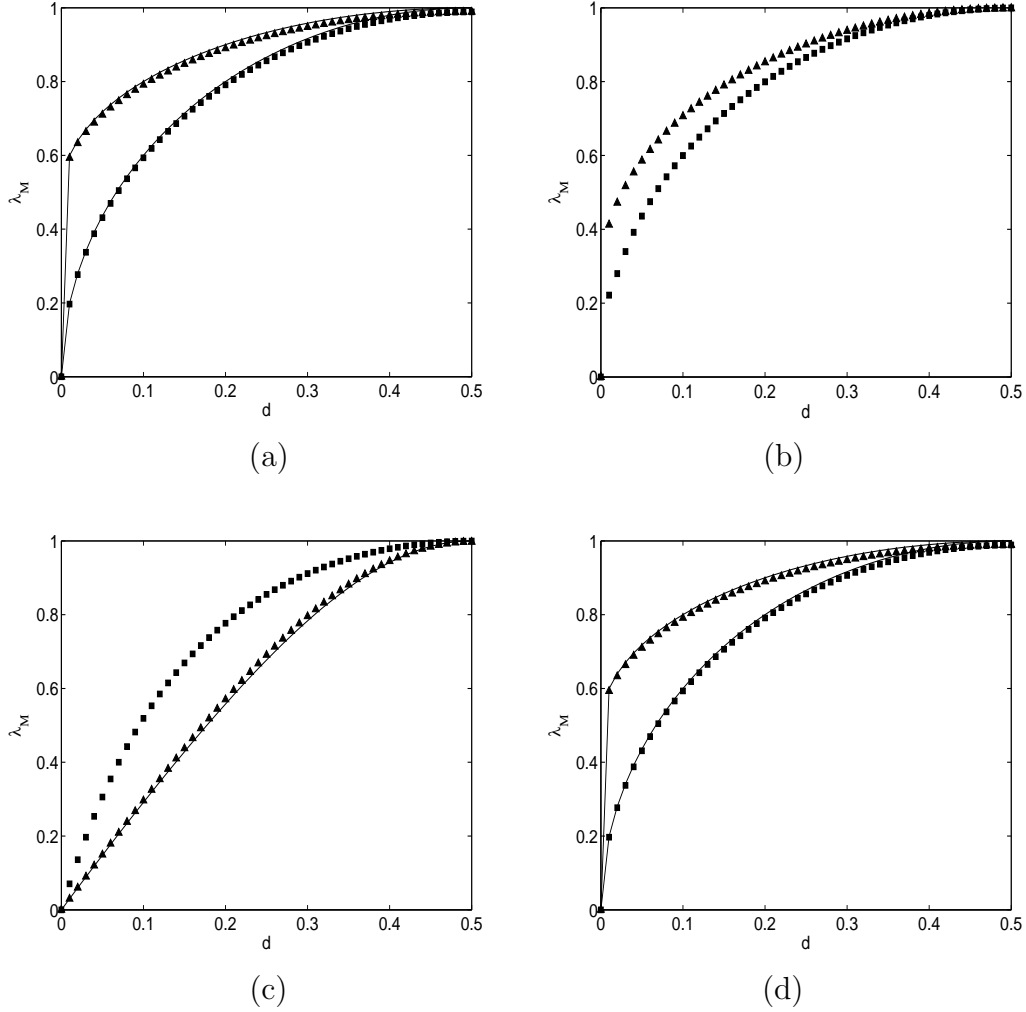


Figure 3: Metapopulation capacity λ_M as a function of the asymmetry factor d for: (a) the island model (triangles) and the linear stepping stone model (squares), (b) the weakly distance-dependent asymmetric model with $\alpha = 1$ (triangles) and $\alpha = 10$ (squares), (c) the strongly distance-dependent asymmetric model with $\alpha = 1$ (triangles) and $\alpha = 10$ (squares), and (d) the grid stepping stone model with horizontal asymmetry in the direction of propagation (triangles) and diagonal asymmetry (squares). The number of patches $n = 100$. The solid curves correspond to theoretical values obtained (or conjectured) for large system size n .

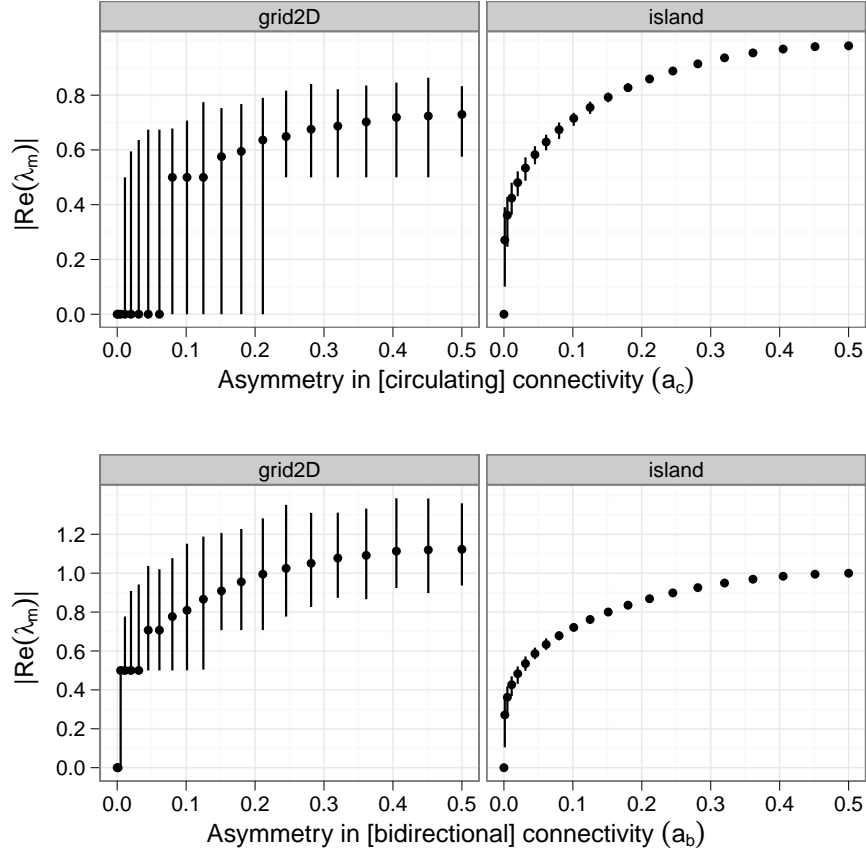


Figure 4: The minimum, median, and maximum value of the metapopulation capacity λ_M as a function of the asymmetry parameters a_b and a_c for the island model and for the stepping stone model considering either bidirectional connection or a circulation system (see method for details). Only real leading eigenvalues were considered for the grid2D case, were excluded 733/21000 complex leading eigenvalues for the bidirectional case, 20/21000 pure-imaginary and 753/21000 complex leading eigenvalues for the circulating case.

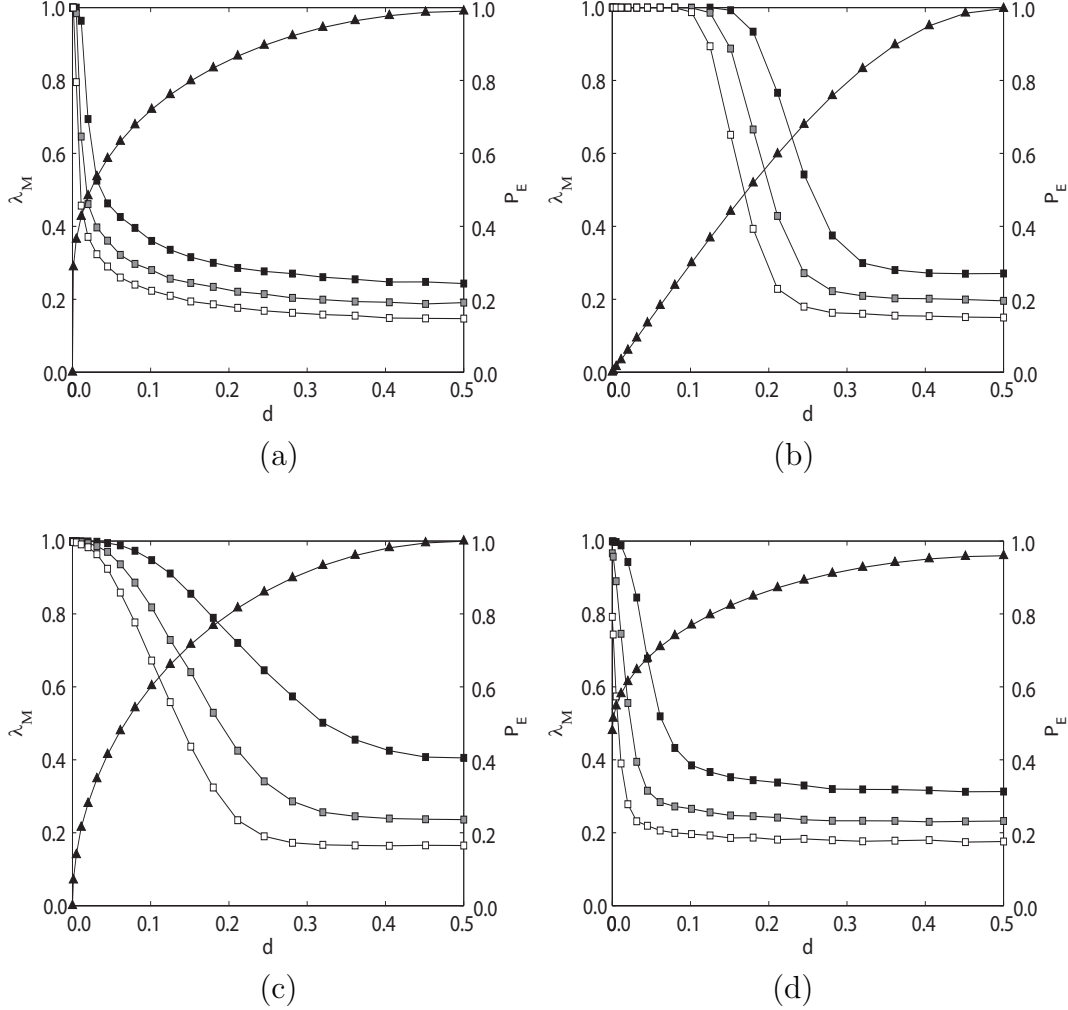


Figure 5: Metapopulation capacity λ_M (triangles) and extinction probability p_E (squares) as a function of the asymmetry factor d and the colonization rate c for (a) the island model, (b) the strongly asymmetric distance-dependent model with $\alpha = 1$, (c) the linear stepping stone model, and (d) the grid stepping stone model with horizontal asymmetry. The number of patches $n = 100$, the number of generations $g = 1000$ and the number of simulations $s = 1000$ (except for the linear stepping stone model with $s = 2500$). In addition, the local extinction rate $e = 0.1$ and the colonization rate $c = 0.4$ (black squares), $c = 0.5$ (gray squares) and $c = 0.6$ (white squares).

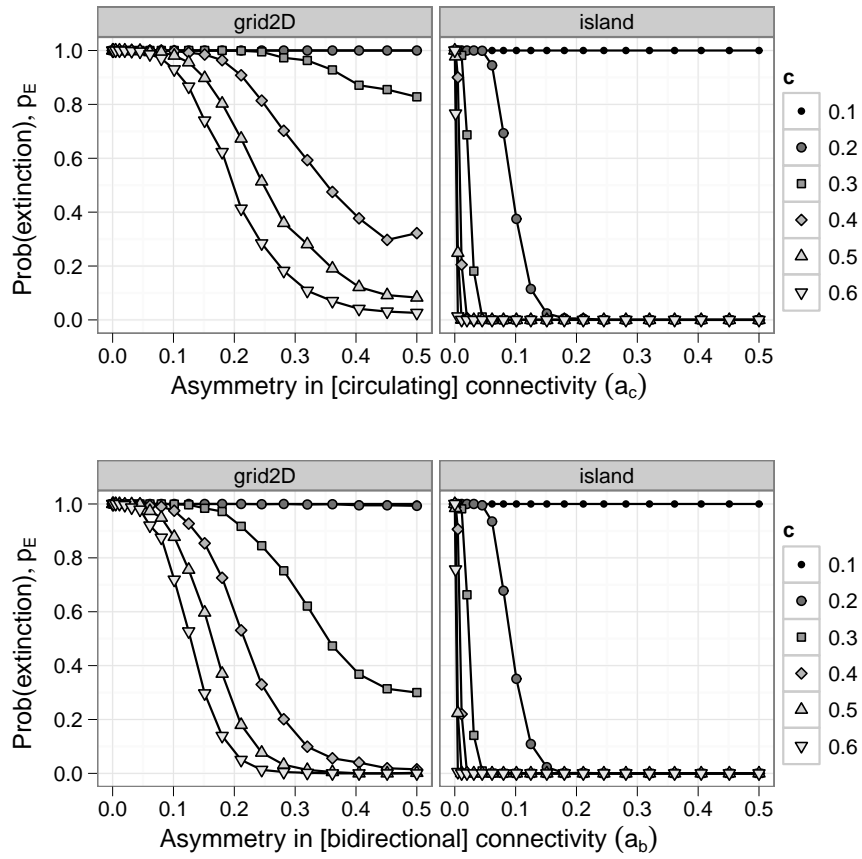


Figure 6: Probability of metapopulation extinction, p_E , as a function of the asymmetry parameter a_b and a_c for the island model and for the stepping stone with locale extinction rate $e=0.1$ and the colonization rate $c = 0.1, 0.2, 0.3, 0.4, 0.5, 0.6$. Dynamics is simulated for 1000 time steps.

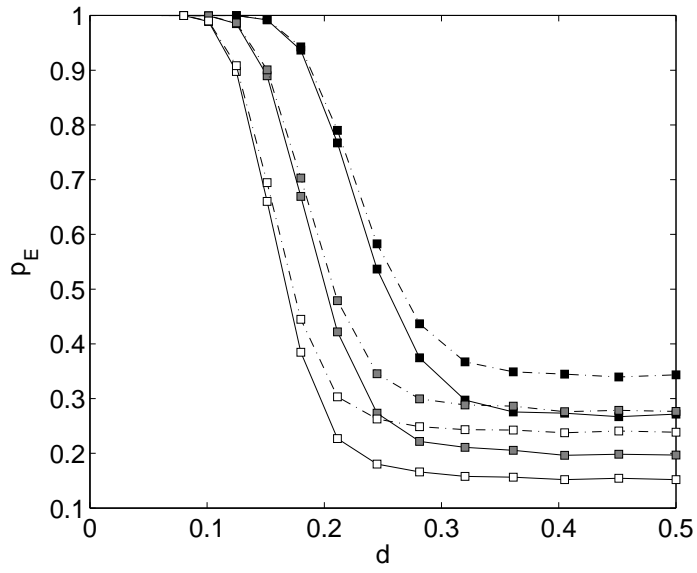


Figure 7: Impact of permuting extinction and recolonization events on extinction probability p_E . The model and parameters here are the same as in Figure 5b. Solid (resp. dotted) lines represent the results obtained when extinctions (resp. recolonizations) are performed first.

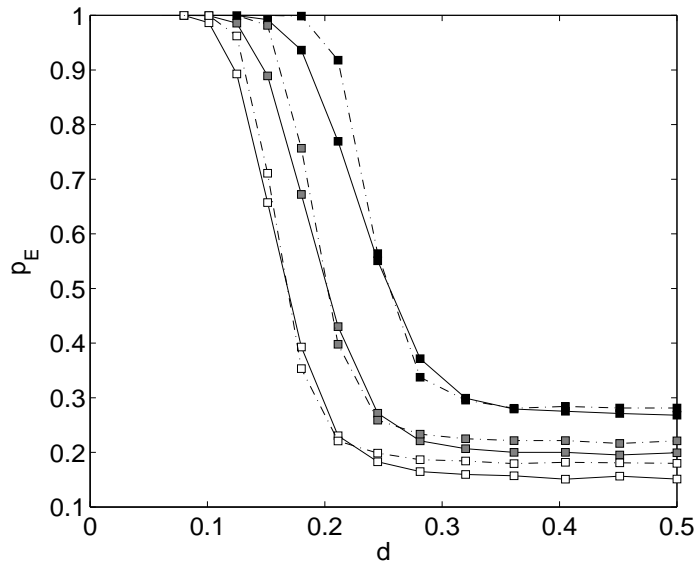


Figure 8: Comparison of predictions obtained by a discrete-time or a continuous-time simulation model. The model and parameters here are the same as in Figure 5b. Solid (resp. dotted) lines represent the results for the discrete-time (resp. continuous-time) model.

1 **Appendix A. Proofs**

2 *Appendix A.1. Linear stepping stone model*

3 We prove here (28). Under the stepping stone model (13), the matrix M may be
 4 rewritten as

$$M = \begin{pmatrix} 0 & d & & 0 \\ 1-d & 0 & d & \\ & 1-d & 0 & \ddots \\ & & \ddots & \ddots & d \\ 0 & & & 1-d & 0 \end{pmatrix} = \sqrt{d(1-d)} \begin{pmatrix} 0 & x & & 0 \\ 1/x & 0 & x & \\ & 1/x & 0 & \ddots \\ & & \ddots & \ddots & x \\ 0 & & & 1/x & 0 \end{pmatrix} \quad (\text{A.1})$$

5 where $x = \sqrt{d/(1-d)}$. Let us now write

$$D_n(\lambda) = \det \begin{pmatrix} -\lambda & x & & 0 \\ 1/x & -\lambda & x & \\ & 1/x & -\lambda & \ddots \\ & & \ddots & \ddots & x \\ 0 & & & 1/x & -\lambda \end{pmatrix} \quad (\text{A.2})$$

6 It follows that $D_1(\lambda) = -\lambda$, $D_2(\lambda) = \lambda^2 - x(1/x) = \lambda^2 - 1$ and expanding the determinant
 7 along the last column for general n gives

$$D_n(\lambda) = -\lambda D_{n-1}(\lambda) - x(1/x) D_{n-2}(\lambda) = -\lambda D_{n-1}(\lambda) - D_{n-2}(\lambda) \quad (\text{A.3})$$

8 By induction, this shows that $D_n(\lambda)$ does actually not depend on x , so the eigenvalues
 9 of the matrices

$$\begin{pmatrix} 0 & x & & 0 \\ 1/x & 0 & x & \\ & 1/x & 0 & \ddots \\ & & \ddots & \ddots & x \\ 0 & & & 1/x & 0 \end{pmatrix} \quad \text{and} \quad \begin{pmatrix} 0 & 1 & & 0 \\ 1 & 0 & 1 & \\ & 1 & 0 & \ddots \\ & & \ddots & \ddots & 1 \\ 0 & & & 1 & 0 \end{pmatrix} \quad (\text{A.4})$$

1 are the same. It is now a well know fact that as $n \rightarrow \infty$, the largest eigenvalue of the
 2 latter matrix converges to 2 (Gray 2006). So as $n \rightarrow \infty$, the largest eigenvalue of M
 3 converges to

$$\lambda_M(d) = 2\sqrt{d(1-d)} \quad (\text{A.5})$$

4 *Appendix A.2. Strongly asymmetric distance-dependent model*

5 We prove here (30). Under the distance-dependent model (19) and when $\alpha = 1$, the
 6 matrix M may be rewritten as $M = d(1-d)X$, where

$$x_{ij} = \begin{cases} d^{j-i-1} & \text{if } i < j \\ (1-d)^{i-j-1} & \text{if } i > j \end{cases} \quad (\text{A.6})$$

7 Now, for any fixed n and as d tends to 0, the matrix X tends to

$$X_0 = \begin{pmatrix} 0 & 1 & & 0 \\ 1 & 0 & 1 & \\ & 1 & 0 & \ddots \\ & & \ddots & \ddots & 1 \\ 1 & & & 1 & 0 \end{pmatrix} \quad (\text{A.7})$$

8 In the following, we prove that for any n , the largest eigenvalue λ_{X_0} of X_0 cannot be
 9 greater than 3, thus proving that as d tends to 0,

$$\lim_{d \rightarrow 0} \frac{\lambda_M(d)}{d} = \lim_{d \rightarrow 0} \frac{d(1-d)\lambda_{X_0}}{d} \leq \lim_{d \rightarrow 0} \frac{3d(1-d)}{d} \leq 3. \quad (\text{A.8})$$

10 or in other words, that $\lambda'_M(0) \leq 3$, which is (30).

11 The fact that $\lambda_{X_0} \leq 3$ is proven as follows. Let $D_n(\lambda)$ and $E_n(\lambda)$ be defined as

$$D_n(\lambda) = \det \begin{pmatrix} -\lambda & 1 & & 0 \\ 1 & -\lambda & 1 & \\ & 1 & -\lambda & \ddots \\ & & \ddots & \ddots & 1 \\ 1 & & & 1 & -\lambda \end{pmatrix} \quad \text{and} \quad E_n(\lambda) = \det \begin{pmatrix} -\lambda & 1 & & 0 \\ 1 & -\lambda & 1 & \\ & 1 & -\lambda & \ddots \\ & & \ddots & -\lambda & 1 \\ 1 & & & 1 & 1 \end{pmatrix} \quad (\text{A.9})$$

1 By expanding the determinant along the last column, the following recurrence relations
 2 are obtained:

$$D_{n+1}(\lambda) = -\lambda D_n(\lambda) - E_n(\lambda) \quad \text{and} \quad E_{n+1}(\lambda) = D_n(\lambda) - E_n(\lambda) \quad (\text{A.10})$$

3 We now make the following claim: if $\lambda > 3$, then for all values of n , $|D_n(\lambda)| \geq |E_n(\lambda)|$
 4 and $D_n(\lambda) E_n(\lambda) < 0$. This implies in particular that if $\lambda > 3$, then for all values of n ,
 5 $D_n(\lambda) \neq 0$, so λ cannot be an eigenvalue of X_0 and therefore $\lambda_{X_0} \leq 3$.

6 *Proof of the claim.* We proceed by induction. Since $D_1(\lambda) = -\lambda$ and $E_1(\lambda) = 1$, it
 7 is clear by assumption that $|D_1(\lambda)| \geq |E_1(\lambda)|$ and $D_1(\lambda) E_1(\lambda) < 0$. Assume now that
 8 $|D_n(\lambda)| \geq |E_n(\lambda)|$ and $D_n(\lambda) E_n(\lambda) < 0$. Then,

$$D_{n+1}(\lambda) E_{n+1}(\lambda) = -\lambda D_n(\lambda)^2 + E_n(\lambda)^2 + (\lambda - 1) D_n(\lambda) E_n(\lambda) < 0 \quad (\text{A.11})$$

9 Besides,

$$|E_{n+1}(\lambda)| = |D_n(\lambda) - E_n(\lambda)| = |D_n(\lambda)| + |E_n(\lambda)| \quad (\text{A.12})$$

10 and

$$|D_{n+1}(\lambda)| = |\lambda D_n(\lambda) + E_n(\lambda)| = |(\lambda + 1) D_n(\lambda) + E_n(\lambda) - D_n(\lambda)| \quad (\text{A.13})$$

11 As $|(\lambda + 1) D_n(\lambda)| \geq |E_n(\lambda) - D_n(\lambda)|$, it is still true by assumption that

$$|D_{n+1}(\lambda)| = |(\lambda + 1) D_n(\lambda)| - |E_n(\lambda) - D_n(\lambda)| \geq 4 |D_n(\lambda)| - |E_{n+1}(\lambda)| \quad (\text{A.14})$$

$$\geq 2(|D_n(\lambda)| + |E_n(\lambda)|) - |E_{n+1}(\lambda)| = 2|E_{n+1}(\lambda)| - |E_{n+1}(\lambda)| = |E_{n+1}(\lambda)| \quad (\text{A.15})$$

12 so the claim is proved.

13 *Appendix A.3. Grid stepping stone model*

14 We prove here (31). In the grid case, the matrix M of the stepping stone model has
 15 the following structure:

$$M = \frac{1}{2} \begin{pmatrix} M' & D & & 0 \\ D & M' & D & \\ & \ddots & \ddots & \ddots \\ & & D & M' & D \\ 0 & & & D & M' \end{pmatrix} \quad (\text{A.16})$$

1 where M' is the matrix of the linear stepping stone model and $D = \text{diag}(1/2, \dots, 1/2)$.
 2 The eigenvalue decomposition of each matrix M' reads $M' = S\Lambda'S^{-1}$, where S is an
 3 invertible matrix and Λ' is the diagonal matrix of eigenvalues of M' . Therefore,

$$M = \frac{1}{2} \begin{pmatrix} S & 0 & & 0 \\ 0 & S & & 0 \\ & \ddots & \ddots & \ddots \\ & & 0 & S & 0 \\ 0 & & & 0 & S \end{pmatrix} \begin{pmatrix} \Lambda' & D & & 0 \\ D & \Lambda' & D & \\ & \ddots & \ddots & \ddots \\ & & D & \Lambda' & D \\ 0 & & & D & \Lambda' \end{pmatrix} \begin{pmatrix} S^{-1} & 0 & & 0 \\ 0 & S^{-1} & & 0 \\ & \ddots & \ddots & \ddots \\ & & 0 & S^{-1} & 0 \\ 0 & & & 0 & S^{-1} \end{pmatrix} \quad (\text{A.17})$$

4 and the eigenvalues of M are the same as those of

$$\Lambda = \frac{1}{2} \begin{pmatrix} \Lambda' & D & & 0 \\ D & \Lambda' & D & \\ & \ddots & \ddots & \ddots \\ & & D & \Lambda' & D \\ 0 & & & D & \Lambda' \end{pmatrix} \quad (\text{A.18})$$

5 Let us denote by $\lambda_M^{2D}(d)$ the largest eigenvalue of M (that is, of Λ) and by $\lambda_M^{1D}(d)$ the
 6 largest eigenvalue of M' (that is, of Λ'). By Geršgorin's discs' argument, we know that

$$\lambda_M^{2D}(d) \leq \frac{1}{2}(\lambda_M^{1D}(d) + 1) \quad (\text{A.19})$$

7 which proves half of the claim. This upper bound is achieved for large system size n :
 8 indeed, if λ is an eigenvalue of the reduced size matrix

$$\tilde{\Lambda} = \frac{1}{2} \begin{pmatrix} \lambda_M^{1D}(d) & 1/2 & & 0 \\ 1/2 & \lambda_M^{1D}(d) & 1/2 & \\ & \ddots & \ddots & \ddots \\ & & 1/2 & \lambda_M^{1D}(d) & 1/2 \\ 0 & & & 1/2 & \lambda_M^{1D}(d) \end{pmatrix} \quad (\text{A.20})$$

9 then it is easily seen that λ is also an eigenvalue of the matrix Λ . As the largest eigenvalue
 10 of $\tilde{\Lambda}$ is known to converge to $\frac{1}{2}(\lambda_M^{1D}(d) + 1)$ for large n (Gray 2006), the claim is proved.